

Measurement of the $e^+e^- \rightarrow \pi^+\pi^- J/\psi$ Cross Section Via Initial-State Radiation at Belle

C. Z. Yuan,¹¹ C. P. Shen,¹¹ P. Wang,¹¹ S. McOnie,³⁹ I. Adachi,⁸ H. Aihara,⁴³ V. Aulchenko,¹ T. Aushev,^{19,14} S. Bahinipati,³ V. Balagura,¹⁴ E. Barberio,²² I. Bedny,¹ U. Bitenc,¹⁵ A. Bondar,¹ A. Bozek,²⁸ M. Bračko,^{21,15} J. Brodzicka,⁸ T. E. Browder,⁷ M.-C. Chang,⁴ P. Chang,²⁷ A. Chen,²⁵ K.-F. Chen,²⁷ W. T. Chen,²⁵ B. G. Cheon,⁶ R. Chistov,¹⁴ I.-S. Cho,⁴⁷ Y. Choi,³⁸ J. Dalseno,²² M. Danilov,¹⁴ M. Dash,⁴⁶ S. Eidelman,¹ S. Fratina,¹⁵ N. Gabyshev,¹ B. Golob,^{20,15} H. Ha,¹⁷ J. Haba,⁸ K. Hayasaka,²³ H. Hayashii,²⁴ M. Hazumi,⁸ D. Heffernan,³² T. Hokuue,²³ Y. Hoshi,⁴¹ W.-S. Hou,²⁷ Y. B. Hsiung,²⁷ H. J. Hyun,¹⁸ T. Iijima,²³ K. Ikado,²³ K. Inami,²³ A. Ishikawa,⁴³ R. Itoh,⁸ Y. Iwasaki,⁸ D. H. Kah,¹⁸ H. Kaji,²³ J. H. Kang,⁴⁷ N. Katayama,⁸ H. Kawai,² T. Kawasaki,³⁰ H. Kichimi,⁸ Y. J. Kim,⁵ K. Kinoshita,³ S. Korpar,^{21,15} P. Križan,^{20,15} P. Krokovny,⁸ R. Kumar,³³ C. C. Kuo,²⁵ A. Kuzmin,¹ Y.-J. Kwon,⁴⁷ S. E. Lee,³⁷ T. Lesiak,²⁸ S.-W. Lin,²⁷ Y. Liu,⁵ D. Liventsev,¹⁴ F. Mandl,¹² D. Marlow,³⁴ A. Matyja,²⁸ T. Medvedeva,¹⁴ W. Mitaroff,¹² K. Miyabayashi,²⁴ H. Miyake,³² H. Miyata,³⁰ Y. Miyazaki,²³ R. Mizuk,¹⁴ T. Mori,²³ Y. Nagasaka,⁹ M. Nakao,⁸ Z. Natkaniec,²⁸ S. Nishida,⁸ O. Nitoh,⁴⁵ S. Ogawa,⁴⁰ T. Ohshima,²³ S. Okuno,¹⁶ S. L. Olsen,⁷ H. Ozaki,⁸ P. Pakhlov,¹⁴ G. Pakhlova,¹⁴ H. Palka,²⁸ H. Park,¹⁸ K. S. Park,³⁸ L. S. Peak,³⁹ L. E. Piilonen,⁴⁶ Y. Sakai,⁸ O. Schneider,¹⁹ J. Schümann,⁸ R. Seidl,^{10,35} K. Senyo,²³ M. E. Sevior,²² M. Shapkin,¹³ H. Shibuya,⁴⁰ J.-G. Shiu,²⁷ B. Shwartz,¹ J. B. Singh,³³ A. Sokolov,¹³ A. Somov,³ M. Starič,¹⁵ T. Sumiyoshi,⁴⁴ F. Takasaki,⁸ M. Tanaka,⁸ G. N. Taylor,²² Y. Teramoto,³¹ I. Tikhomirov,¹⁴ S. Uehara,⁸ Y. Unno,⁶ S. Uno,⁸ Y. Usov,¹ G. Varner,⁷ K. E. Varvell,³⁹ K. Vervink,¹⁹ S. Villa,¹⁹ A. Vinokurova,¹ C. C. Wang,²⁷ C. H. Wang,²⁶ X. L. Wang,¹¹ Y. Watanabe,¹⁶ E. Won,¹⁷ B. D. Yabsley,³⁹ A. Yamaguchi,⁴² Y. Yamashita,²⁹ C. C. Zhang,¹¹ Z. P. Zhang,³⁶ V. Zhilich,¹ V. Zhulanov,¹ and A. Zupanc¹⁵

(Belle Collaboration)

¹*Budker Institute of Nuclear Physics, Novosibirsk*²*Chiba University, Chiba*³*University of Cincinnati, Cincinnati, Ohio 45221*⁴*Department of Physics, Fu Jen Catholic University, Taipei*⁵*The Graduate University for Advanced Studies, Hayama*⁶*Hanyang University, Seoul*⁷*University of Hawaii, Honolulu, Hawaii 96822*⁸*High Energy Accelerator Research Organization (KEK), Tsukuba*⁹*Hiroshima Institute of Technology, Hiroshima*¹⁰*University of Illinois at Urbana-Champaign, Urbana, Illinois 61801*¹¹*Institute of High Energy Physics, Chinese Academy of Sciences, Beijing*¹²*Institute of High Energy Physics, Vienna*¹³*Institute of High Energy Physics, Protvino*¹⁴*Institute for Theoretical and Experimental Physics, Moscow*¹⁵*J. Stefan Institute, Ljubljana*¹⁶*Kanagawa University, Yokohama*¹⁷*Korea University, Seoul*¹⁸*Kyungpook National University, Taegu*¹⁹*Swiss Federal Institute of Technology of Lausanne, EPFL, Lausanne*²⁰*University of Ljubljana, Ljubljana*²¹*University of Maribor, Maribor*²²*University of Melbourne, School of Physics, Victoria 3010*²³*Nagoya University, Nagoya*²⁴*Nara Women's University, Nara*²⁵*National Central University, Chung-li*²⁶*National United University, Miao Li*²⁷*Department of Physics, National Taiwan University, Taipei*²⁸*H. Niewodniczanski Institute of Nuclear Physics, Krakow*²⁹*Nippon Dental University, Niigata*³⁰*Niigata University, Niigata*³¹*Osaka City University, Osaka*³²*Osaka University, Osaka*³³*Panjab University, Chandigarh*³⁴*Princeton University, Princeton, New Jersey 08544*

³⁵*RIKEN BNL Research Center, Upton, New York 11973*³⁶*University of Science and Technology of China, Hefei*³⁷*Seoul National University, Seoul*³⁸*Sungkyunkwan University, Suwon*³⁹*University of Sydney, Sydney, New South Wales*⁴⁰*Toho University, Funabashi*⁴¹*Tohoku Gakuin University, Tagajo*⁴²*Tohoku University, Sendai*⁴³*Department of Physics, University of Tokyo, Tokyo*⁴⁴*Tokyo Metropolitan University, Tokyo*⁴⁵*Tokyo University of Agriculture and Technology, Tokyo*⁴⁶*Virginia Polytechnic Institute and State University, Blacksburg, Virginia 24061*⁴⁷*Yonsei University, Seoul*

(Received 17 July 2007; published 2 November 2007)

The cross section for $e^+e^- \rightarrow \pi^+\pi^-J/\psi$ between 3.8 and 5.5 GeV/ c^2 is measured using a 548 fb $^{-1}$ data sample collected on or near the $Y(4S)$ resonance with the Belle detector at KEKB. A peak near 4.25 GeV/ c^2 , corresponding to the so called $Y(4260)$, is observed. In addition, there is another cluster of events at around 4.05 GeV/ c^2 . A fit using two interfering Breit-Wigner shapes describes the data better than one that uses only the $Y(4260)$, especially for the lower-mass side of the 4.25 GeV enhancement.

DOI: 10.1103/PhysRevLett.99.182004

PACS numbers: 13.66.Bc, 13.25.Gv, 14.40.Gx

In a recent study of initial-state radiation (ISR) events of the type, $e^+e^- \rightarrow \gamma_{\text{ISR}}\pi^+\pi^-J/\psi$, the BABAR Collaboration observed an accumulation of events near 4.26 GeV/ c^2 in the $\pi^+\pi^-J/\psi$ invariant mass distribution and attributed it to a possible new resonance that they dubbed the $Y(4260)$ [1]. This observation was confirmed by the CLEO experiment using a similar technique with a data sample collected at the $Y(4S)$ peak [2]. The CLEO Collaboration also collected a 13.2 pb $^{-1}$ data sample at $\sqrt{s} = 4.26$ GeV, and reported signals for $\pi^+\pi^-J/\psi$, $\pi^0\pi^0J/\psi$, and K^+K^-J/ψ with cross sections that are significantly higher than those measured at other nearby energies [3].

Since the $Y(4260)$ resonance is produced via e^+e^- annihilation accompanied with initial-state radiation, its $J^{\text{PC}} = 1^{--}$. However, the properties of the observed peak are rather different from those of other known $J^{\text{PC}} = 1^{--}$ charmonium states in the same mass range, such as $\psi(4040)$, $\psi(4160)$, and $\psi(4415)$. Since it is well above the $D\bar{D}$ threshold, it is expected to decay predominantly into $D^{(*)}\bar{D}^{(*)}$ final states. The partial width for the $\pi\pi J/\psi$ final state is expected to be a small fraction of the total. In fact, the $Y(4260)$ shows an unusually strong coupling to the $\pi\pi J/\psi$ final state while no significant enhancement is observed in $D^{(*)}\bar{D}^{(*)}$ final states [4]. In a fit to the total hadronic cross sections measured by the BES experiment [5,6] for \sqrt{s} between 3.7 and 5.0 GeV, Mo *et al.* set an upper limit on $\Gamma_{e^+e^-}$ for the $Y(4260)$ to be less than 580 eV at 90% confidence level (C.L.) [7]. This implies that its branching fraction to $\pi\pi J/\psi$ is greater than 1.3% at 90% C.L. These properties have triggered many models to explain the $Y(4260)$ as an exotic state, such as a four-quark state, a molecular state, or a quark-gluon hybrid [8].

In the analysis reported here, we use a 548 fb $^{-1}$ data sample collected with the Belle detector [9] operating at the KEKB asymmetric-energy e^+e^- (3.5 on 8 GeV) col-

lider [10] to investigate the $\pi^+\pi^-J/\psi$ final state produced via ISR. About 90% of the data were collected at the $Y(4S)$ resonance ($\sqrt{s} = 10.58$ GeV), and about 10% were taken at a center-of-mass (c.m.) energy that is 60 MeV below the $Y(4S)$ peak. The measurement in this Letter uses an improved efficiency for detecting ISR events, and supersedes the preliminary results in Ref. [11], which confirmed the structure near 4.26 GeV/ c^2 .

For Monte Carlo (MC) simulations of the ISR process, we generate signal events with the PHOKHARA program [12]. In this program, after one or two photons are emitted, the lower energy e^+e^- pair forms a resonance X that subsequently decays to $\pi^+\pi^-J/\psi$ with the J/ψ decaying either to e^+e^- or to $\mu^+\mu^-$. In the $X \rightarrow \pi^+\pi^-J/\psi$ generation, we use pure S waves between the $\pi\pi$ system and the J/ψ , as well as between the π^+ and π^- ; this is in agreement with the experimental results [1,13]. The $\pi^+\pi^-$ invariant mass distributions are generated according to phase space. For $\psi(2S) \rightarrow \pi^+\pi^-J/\psi$, which we use as a calibration process, we use the decay properties that have been measured with high precision [13].

For candidate events, we require the number of charged tracks to be four and net charge to be zero. For these tracks, the impact parameters perpendicular to and along the beam direction with respect to the interaction point are required to be less than 0.5 and 4 cm, respectively, and transverse momentum is restricted to be higher than 0.1 GeV/ c . For each charged track, information from different detector subsystems is combined to form a likelihood for each particle species (i), \mathcal{L}_i [14]. Tracks with $\mathcal{R}_K = \frac{\mathcal{L}_K}{\mathcal{L}_K + \mathcal{L}_\pi} < 0.4$ are identified as pions with an efficiency of about 95% for the tracks of interest. Similar likelihood ratios are formed for electron and muon identification. For electrons from $J/\psi \rightarrow e^+e^-$, one track should have $\mathcal{R}_e > 0.95$ and the other $\mathcal{R}_e > 0.05$; for muons from $J/\psi \rightarrow \mu^+\mu^-$, at

least one track is required to have $\mathcal{R}_\mu > 0.95$; in cases where one of the tracks has no muon identification (ID) information, the polar angles of the two muon tracks in the $\pi^+\pi^-\mu^+\mu^-$ c.m. system are required to satisfy $|\cos\theta_\mu| < 0.7$ based on a comparison between data and MC simulation. Lepton ID efficiency is about 90% for $J/\psi \rightarrow e^+e^-$ and 87% for $J/\psi \rightarrow \mu^+\mu^-$. Events with γ conversions are removed by requiring $\mathcal{R}_e < 0.75$ for the $\pi^+\pi^-$ tracks. For the $J/\psi \rightarrow e^+e^-$ mode, γ -conversion events are further removed by requiring the $\pi^+\pi^-$ invariant mass to be greater than $0.35 \text{ GeV}/c^2$.

The detection of the ISR photon is not required; instead, we identify ISR events by the requirement $|M_{\text{rec}}^2| < 2.0 \text{ (GeV}/c^2)^2$, where M_{rec}^2 is the square of the mass that is recoiling against the four charged tracks.

Clear J/ψ signals are observed in both decay modes. We define a J/ψ signal region as $3.06 \text{ GeV}/c^2 < m_{\ell^+\ell^-} < 3.14 \text{ GeV}/c^2$ (the mass resolution is about $17 \text{ MeV}/c^2$), and J/ψ mass sidebands as $m_{\ell^+\ell^-} \in [2.91, 3.03] \text{ GeV}/c^2$ or $m_{\ell^+\ell^-} \in [3.17, 3.29] \text{ GeV}/c^2$; the latter are 3 times as wide as the signal region.

Figure 1 shows the $\pi^+\pi^-\ell^+\ell^-$ invariant mass [15] distribution after the above selection, together with the background estimated from the J/ψ mass sidebands. In addition to a huge $\psi(2S)$ signal, there is a clear enhancement at $4.25 \text{ GeV}/c^2$ similar to that observed by the BABAR Collaboration [1]. In addition, there is a clustering of events around $4.05 \text{ GeV}/c^2$ that is significantly above the background level. It is evident in the figure that the background estimated from the J/ψ sidebands agrees well with the level of the selected events in the high $\pi^+\pi^-\ell^+\ell^-$ invariant mass region. A study of events in the $|M_{\text{rec}}^2| > 1 \text{ (GeV}/c^2)^2$ region, which is depleted in signal events, supports this conclusion. The backgrounds not in the sidebands, including: (1) $\pi^+\pi^-J/\psi$, with J/ψ decays into final states other than lepton pairs; (2) XJ/ψ ,

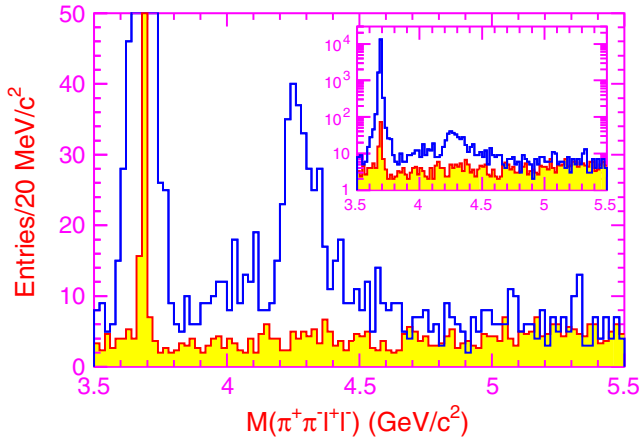


FIG. 1 (color online). Invariant mass distribution of $\pi^+\pi^-\ell^+\ell^-$. The blank histograms represent the selected data, and the shaded histograms are the normalized sidebands. The inset shows the distribution with a logarithmic vertical scale.

with X not being $\pi^+\pi^-$, such as K^+K^- and $\pi^+\pi^-\pi^0$, are found from MC simulation to be less than one event per $20 \text{ MeV}/c^2$ bin at 90% C.L. according to the CLEO measurements [3] and are neglected. The production of $\pi^+\pi^-J/\psi$ from non-ISR processes, such as $e^+e^- \rightarrow \gamma\gamma^*\gamma^* \rightarrow \gamma\rho^0J/\psi$, is computed to be small [16] and is neglected.

The data points in Figs. 2(a) and 2(b) show the background-subtracted M_{rec}^2 distribution and the polar angle distribution of the $\pi^+\pi^-J/\psi$ system in the e^+e^- c.m. system for the selected $\pi^+\pi^-J/\psi$ events with invariant mass between 3.8 and $4.6 \text{ GeV}/c^2$. The data agree well with the MC simulation, indicating that the signal events are produced via ISR.

We estimate the signal significance of the clusters at $4.05 \text{ GeV}/c^2$ and $4.25 \text{ GeV}/c^2$ by comparing the numbers of signal events (number of observed events in the J/ψ signal window minus the number of J/ψ -sideband-estimated background events) with their statistical uncertainties. For events with $m_{\pi^+\pi^-\ell^+\ell^-} \in [3.80, 4.15] \text{ GeV}/c^2$, we have $n^{\text{sig}}(4.05) = 120 \pm 14$, which is more than 8σ from zero assuming a Gaussian error, while for events with $m_{\pi^+\pi^-\ell^+\ell^-} \in [4.15, 4.60] \text{ GeV}/c^2$, we have $n^{\text{sig}}(4.25) = 324 \pm 21$, which is more than 15σ from zero.

The $e^+e^- \rightarrow \pi^+\pi^-J/\psi$ cross section for each $\pi^+\pi^-J/\psi$ mass bin is computed with

$$\sigma_i = \frac{n_i^{\text{obs}} - n_i^{\text{bkg}}}{\varepsilon_i \mathcal{L}_i \mathcal{B}(J/\psi \rightarrow \ell^+\ell^-)},$$

where n_i^{obs} , n_i^{bkg} , ε_i , and \mathcal{L}_i are the number of events observed in data, the number of background events determined from the J/ψ sidebands, the efficiency, and the effective luminosity [17] in the i th $\pi^+\pi^-J/\psi$ mass bin, respectively; $\mathcal{B}(J/\psi \rightarrow \ell^+\ell^-) = 11.87\%$ is taken from Ref. [18]. The resulting cross sections are shown in Fig. 3, where the error bars indicate the combined statisti-

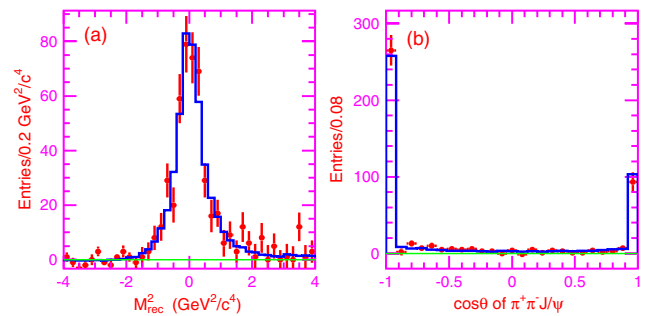


FIG. 2 (color online). M_{rec}^2 distribution (a) and the polar angle distribution of the $\pi^+\pi^-J/\psi$ system in the e^+e^- c.m. frame (b) for the selected $\pi^+\pi^-J/\psi$ events with invariant masses between 3.8 and $4.6 \text{ GeV}/c^2$. The background from J/ψ mass sidebands has been subtracted, and the selection criterion applied to the M_{rec}^2 has been relaxed in (a). The points with error bars are data, compared with MC simulation (solid histograms).

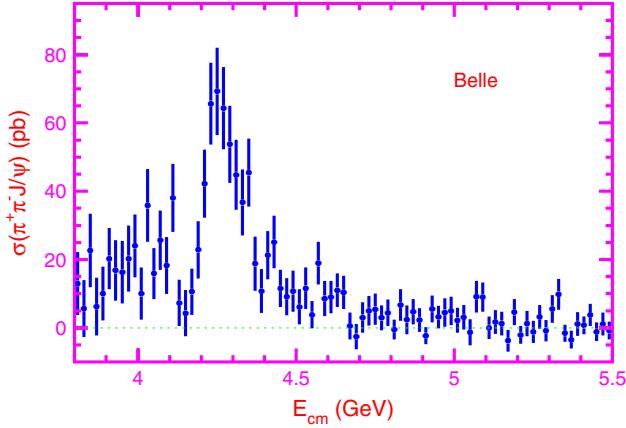


FIG. 3 (color online). The measured $e^+e^- \rightarrow \pi^+\pi^- J/\psi$ cross section for c.m. energies between 3.8 and 5.5 GeV. The errors are statistical only.

cal errors of the signal plus background events. Our measurement at 4.26 GeV/ c^2 agrees well with *BABAR*'s and *CLEO*'s results [1,3].

The sources of the systematic errors for the cross section measurement are listed in Table I. The particle ID uncertainty, measured using the $\psi(2S)$ events in the same data sample, is 3.0%; the uncertainty in the tracking efficiency for tracks with angles and momenta characteristic of signal events is about 1% per track, and is additive; efficiency uncertainties associated with the J/ψ mass and M_{rec}^2 requirements are also determined from a study of the very pure $\psi(2S) \rightarrow \pi^+\pi^- J/\psi$ event sample. In this study we find that the detection efficiency is lower than that inferred from the MC simulation by $(2.5 \pm 0.4)\%$. A correction factor is applied to the final results and 0.4% is included in the systematic error. Belle measures the luminosity with a precision of 1.4% using wide angle Bhabha events, and the uncertainty of the ISR photon radiator is 0.1% [17]. The main uncertainty of the PHOKHARA [12] generator is due to the modeling of the $\pi^+\pi^-$ mass spectrum. Figure 4 shows the $\pi^+\pi^-$ invariant mass distributions of events for three $m_{\pi^+\pi^- J/\psi}$ regions, [3.8, 4.2], [4.2, 4.4], and [4.4, 4.6] (unit

TABLE I. Systematic errors in the cross section measurement. They are common for all data points.

Source	Relative error (%)
Particle ID	3.0
Tracking	4
J/ψ mass and M_{rec}^2 selection	0.4
Integrated luminosity	1.4
$m_{\pi^+\pi^-}$ distribution	5
Trigger efficiency	1
Branching fractions	1
MC statistics	1
Sum in quadrature	7.5

in GeV/ c^2). The $\pi^+\pi^-$ invariant mass distribution for events around 4.25 GeV/ c^2 differs significantly from phase space; for other energy ranges the agreement with phase space is better. Simulations with modified $\pi^+\pi^-$ invariant mass distributions yield efficiencies that are higher by 2%–5% for $m_{\pi^+\pi^- J/\psi}$ below 4.4 GeV/ c^2 . This is not corrected for in the analysis, but is taken as the systematic error (conservatively assigned as 5%) for all $\pi^+\pi^- J/\psi$ mass values. The selected events have four charged tracks and 16%–25% of them have a detected high energy ISR photon. According to the MC simulation, the trigger efficiency for these events is around 98%, with an uncertainty that is smaller than 1%. The uncertainty of $\mathcal{B}(J/\psi \rightarrow \ell^+\ell^-) = \mathcal{B}(J/\psi \rightarrow e^+e^-) + \mathcal{B}(J/\psi \rightarrow \mu^+\mu^-)$ is taken as 1% by linearly adding the errors of the world averages for the e^+e^- and $\mu^+\mu^-$ modes [18]. Finally the MC statistical error on the efficiency is 1%. We assume all the sources are independent and add them in quadrature, resulting in a total systematic error on the cross section of 7.5%.

As a validation of our analysis, we measure the $\psi(2S)$ cross section with the same selection criteria. Here 15 444 $\psi(2S)$ events survive the selection and the MC-determined detection efficiency is 5.13%. This corresponds to $\sigma(\psi(2S)) = (15.42 \pm 0.12 \pm 0.89)$ pb at the $Y(4S)$ resonance or $\Gamma(\psi(2S) \rightarrow e^+e^-) = (2.54 \pm 0.02 \pm 0.15)$ keV, where the first error is statistical and the second systematic. This measurement agrees well with the world average value of (2.48 ± 0.06) keV [18]. The $\psi(2S)$ mass determined from the data indicates the $\pi^+\pi^-\ell^+\ell^-$ invariant mass is measured with a precision of ± 0.6 MeV/ c^2 .

An unbinned maximum likelihood fit is applied to the $\pi^+\pi^-\ell^+\ell^-$ mass spectrum in Fig. 1. Here the theoretical shape is multiplied by the efficiency and effective luminosity, which are functions of the $\pi^+\pi^-\ell^+\ell^-$ invariant mass. Since there are two clusters of events in the mass distribution, we fit it with two coherent Breit-Wigner (BW) resonance functions ($R1, R2$) assuming there is no continuum production of $e^+e^- \rightarrow \pi^+\pi^- J/\psi$. In the fit, the background term is fixed at the level obtained from a linear fit to the sideband data, contributions from the $\psi(2S)$ and $\psi(3770)$ resonance tails (added incoherently) are estimated using world average values for their parameters [18] and fixed, and the widths of the resonances are assumed to be constant. A three-body decay phase-space factor is applied. The MC-determined mass resolution is less than 5 MeV/ c^2 over the full mass range. This is small compared to the widths of the resonances in our study and is ignored.

Figure 5 shows the fit results; there are two solutions with equally good fit quality. The masses and widths of the resonances are the same for both solutions; the partial widths to e^+e^- and the relative phase between them are different (see Table II) [19]. The interference is constructive for one solution and destructive for the other. The

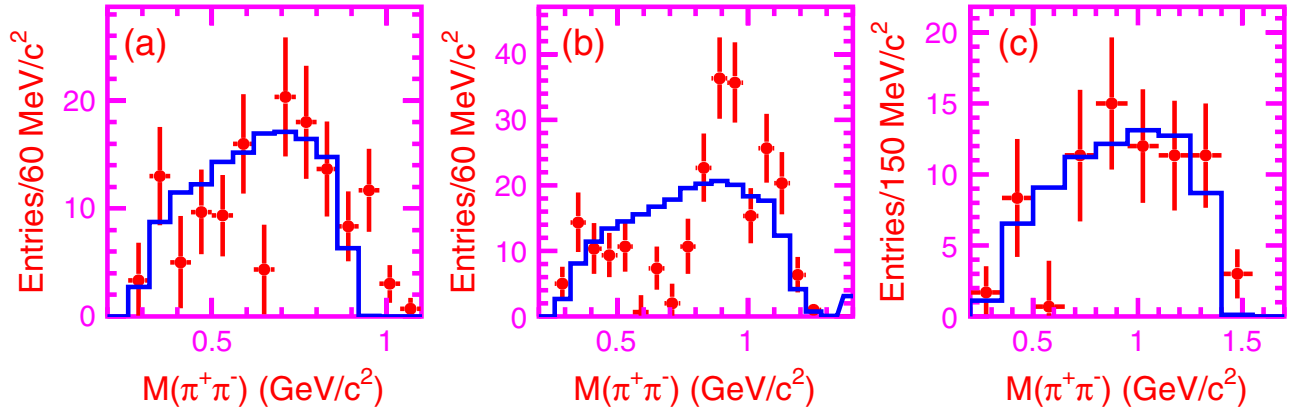


FIG. 4 (color online). The $\pi^+\pi^-$ invariant mass distribution of events for different $\pi^+\pi^-J/\psi$ mass regions. (a) $m_{\pi^+\pi^-J/\psi} \in [3.8, 4.2]$ GeV/c^2 , (b) $m_{\pi^+\pi^-J/\psi} \in [4.2, 4.4]$ GeV/c^2 , and (c) $m_{\pi^+\pi^-J/\psi} \in [4.4, 4.6]$ GeV/c^2 . The points with error bars are pure signal events, the histograms are MC simulations made using phase-space distributions.

systematic errors come from the absolute mass scale, the detection efficiency, the background estimation, the phase-space factor, and the parametrization of the resonances. The quality of the fit assessed from the binned distribution of Fig. 5 is $\chi^2/ndf = 81/78$, corresponding to a C.L. of 38%. The statistical significance of the structure around 4.05 GeV/c^2 is estimated to be 7.4σ from the change in likelihood value when the BW resonance representing it is removed from the fit. Although the mass of the first resonance is close to that of the $\psi(4040)$, the fitted width is much wider than its world average [18] value (80 ± 10 MeV/c^2). The mass of the second resonance is higher than that of the $\psi(4160)$. Changes of resonance parameters that occur when we fit with a coherent $\psi(2S)$ tail, a

coherent or incoherent nonresonance term, an energy-dependent total width, or a cascade two-body phase-space factor dominate the systematic errors listed in Table II; the significance of the R1 signal is greater than 5σ in all of the fitting scenarios that are considered. If we use the same functional form as *BABAR* (a single BW resonance with an incoherent second-order polynomial background term) we find $M = 4263 \pm 6$ MeV/c^2 , $\Gamma_{\text{tot}} = 126 \pm 18$ MeV/c^2 , and $\mathcal{B}(\pi^+\pi^-J/\psi)\Gamma_{e^+e^-} = 9.7 \pm 1.1$ eV/c^2 , consistent with their results [1].

In summary, the $e^+e^- \rightarrow \pi^+\pi^-J/\psi$ cross section is measured for the c.m. energy range $\sqrt{s} = 3.8$ to 5.5 GeV . There are two significant enhancements: one near 4.25 GeV , consistent with the results of Refs. [1,2], and another near 4.05 GeV , which has not previously been observed. We note that these enhancements are close to $D^{(*)}\bar{D}^{(*)}$ thresholds, where coupled-channel effects and rescattering may affect the cross section [20]. If we nevertheless represent the cross section using interfering BW terms, a second term [in addition to the $Y(4260)$] substantially improves the fit. In particular, the lower-mass side of

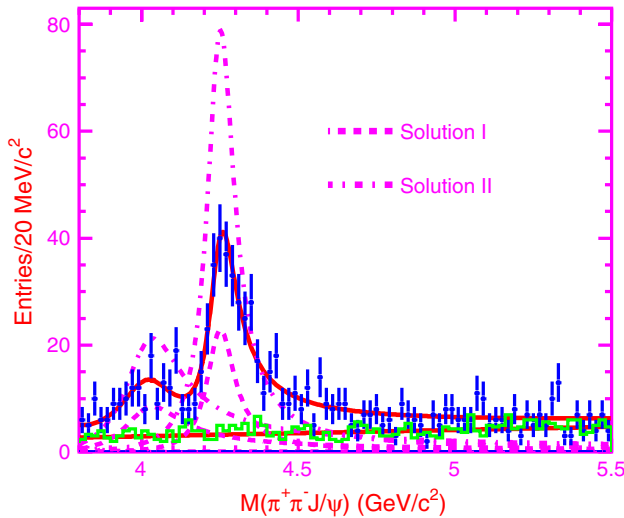


FIG. 5 (color online). Fit to the $\pi^+\pi^-J/\psi$ mass spectrum with two coherent resonances. The curves show the best fit and the contribution from each component. The dashed curves are for solution I, and the dot-dashed curves for solution II. The histogram shows the scaled sideband distribution.

TABLE II. Fit results of the $\pi^+\pi^-J/\psi$ invariant mass spectrum. The first errors are statistical and the second systematic. M , Γ_{tot} , and $\mathcal{B} \cdot \Gamma_{e^+e^-}$ are the mass (in MeV/c^2), total width (in MeV/c^2), product of the branching fraction to $\pi^+\pi^-J/\psi$ and the e^+e^- partial width (in eV/c^2), respectively. ϕ is the relative phase between the two resonances (in degrees).

Parameters	Solution I	Solution II
$M(R1)$	$4008 \pm 40^{+114}_{-28}$	
$\Gamma_{\text{tot}}(R1)$	$226 \pm 44 \pm 87$	
$\mathcal{B}\Gamma_{e^+e^-}(R1)$	$5.0 \pm 1.4^{+6.1}_{-0.9}$	$12.4 \pm 2.4^{+14.8}_{-1.1}$
$M(R2)$	$4247 \pm 12^{+17}_{-32}$	
$\Gamma_{\text{tot}}(R2)$	$108 \pm 19 \pm 10$	
$\mathcal{B}\Gamma_{e^+e^-}(R2)$	$6.0 \pm 1.2^{+4.7}_{-0.5}$	$20.6 \pm 2.3^{+9.1}_{-1.7}$
ϕ	$12 \pm 29^{+7}_{-98}$	$-111 \pm 7^{+28}_{-31}$

the 4.25 GeV enhancement is better reproduced. The parameters that are obtained from this two-term fit do not correspond to those of any of the excited ψ states currently listed in Refs. [18,21].

We express sincere thanks to H. Czyż for helpful discussions on the generator. We thank the KEKB group for excellent operation of the accelerator, the KEK cryogenics group for efficient solenoid operations, and the KEK computer group and the NII for valuable computing and SuperSINET network support. We acknowledge support from MEXT and JSPS (Japan); ARC and DEST (Australia); NSFC, KIP of CAS, and 100 Talents Program of CAS (China); DST (India); MOEHRD, KOSEF, and KRF (Korea); KBN (Poland); MES and RFAAE (Russia); ARRS (Slovenia); SNSF (Switzerland); NSC and MOE (Taiwan); and DOE (USA).

-
- [1] B. Aubert *et al.* (BABAR Collaboration), Phys. Rev. Lett. **95**, 142001 (2005).
- [2] Q. He *et al.* (CLEO Collaboration), Phys. Rev. D **74**, 091104(R) (2006).
- [3] T.E. Coan *et al.* (CLEO Collaboration), Phys. Rev. Lett. **96**, 162003 (2006).
- [4] G. Pakhlova *et al.* (Belle Collaboration), Phys. Rev. Lett. **98**, 092001 (2007).
- [5] J.Z. Bai *et al.* (BES Collaboration), Phys. Rev. Lett. **84**, 594 (2000).
- [6] J.Z. Bai *et al.* (BES Collaboration), Phys. Rev. Lett. **88**, 101802 (2002).
- [7] X.H. Mo *et al.*, Phys. Lett. B **640**, 182 (2006).
- [8] See the recent review by E. S. Swanson, Phys. Rep. **429**, 243 (2006).
- [9] A. Abashian *et al.* (Belle Collaboration), Nucl. Instrum. Methods Phys. Res., Sect. A **479**, 117 (2002).
- [10] S. Kurokawa and E. Kikutani, Nucl. Instrum. Methods Phys. Res., Sect. A **499**, 1 (2003), and other papers included in this volume.
- [11] K. Abe *et al.* (Belle Collaboration), arXiv:hep-ex/0612006.
- [12] G. Rodrigo *et al.*, Eur. Phys. J. C **24**, 71 (2002).
- [13] J.Z. Bai *et al.* (BES Collaboration), Phys. Rev. D **62**, 032002 (2000).
- [14] E. Nakano, Nucl. Instrum. Methods Phys. Res., Sect. A **494**, 402 (2002).
- [15] In this Letter, $m_{\pi^+\pi^-\ell^+\ell^-} - m_{\ell^+\ell^-} + m_{J/\psi}$ is used instead of the invariant mass of the four final state particles to improve the mass resolution. Here $m_{J/\psi}$ is the nominal mass of J/ψ .
- [16] M. Davier, M.E. Peskin, and A. Snyder, arXiv:hep-ph/0606155.
- [17] E. A. Kuraev and V.S. Fadin, Yad. Fiz. **41**, 733 (1985) [Sov. J. Nucl. Phys. **41**, 466 (1985)].
- [18] W.-M. Yao *et al.* (Particle Data Group), J. Phys. G **33**, 1 (2006).
- [19] Considering the correlation between $\mathcal{B}(\pi^+\pi^-J/\psi) \cdot \Gamma_{e^+e^-}$ and Γ_{tot} , we get $\mathcal{B}(\pi^+\pi^-J/\psi) \cdot \mathcal{B}(e^+e^-) = (2.2 \pm 0.7_{-0.4}^{+2.5}) \times 10^{-8}$ and $(5.5 \pm 1.1_{-0.7}^{+4.2}) \times 10^{-8}$ for R1 and R2, respectively, for solution I; and $\mathcal{B}(\pi^+\pi^-J/\psi) \cdot \mathcal{B}(e^+e^-) = (5.5 \pm 1.5_{-1.5}^{+7.0}) \times 10^{-8}$ and $(19.1 \pm 2.4_{-2.3}^{+8.3}) \times 10^{-8}$ for R1 and R2, respectively, for solution II.
- [20] M. B. Voloshin, arXiv:hep-ph/0602233.
- [21] M. Ablikim *et al.* (BES Collaboration), arXiv:0705.4500.